

PROCEEDINGS**SDSS data motivates reassessment of Λ CDM cosmology**

Alexander F. Mayer*

¹IWARA2018 – 8th International Workshop
on Astronomy & Relativistic Astrophysics,
Ollantaytambo, Peru

Correspondence

*Alexander Franklin Mayer

Email: amayer@alum.mit.edu

The objective, statistical nature of SDSS astrophysical datasets, which were not driven by any theoretical agenda, reveal false and misleading prior measurements (e.g., redshift-distance) driven by confirmation bias in the context of such agendas. SDSS theta-z, redshift-magnitude (both spectroscopic and photometric pipelines), and galaxy population-density data are shown to conflict with the Λ CDM standard cosmological model. However, all four of these distinct and independent data sets are similarly consistent with a new cosmological model that revives de Sitter’s 1917 solution to the field equations, long thought to entail an “empty universe.” That new model, which represents a paradigm shift in cosmology, derives from considerations of symmetry and local proper time modeled as a geometric object, motivated by Minkowski (1909). The confrontation of all new predictive equations with corresponding SDSS data sets, using no free parameters, definitively resolves the modern quandary of astrophysical observables interpreted as accelerating cosmic expansion induced by ‘dark energy.’ The canonical idea of a non-relativistic universal time coordinate (i.e., ~ 13.7 Gyr of ‘Cosmic Time’ from initial singularity) is supplanted by a relativistic, strictly-local time coordinate involving no such inscrutable singularity.

KEYWORDS:

cosmology, general relativity, de Sitter, SDSS

1 | INTRODUCTION

At the time of this paper’s submission, the current cosmological paradigm, which defines guidelines for what constitutes legitimate contributions to the field, is the Λ CDM standard cosmological model [Scott \(2018\)](#). The fundamental premise of that model is uniform and isotropic expansion of space from a primordial singularity ~ 13.7 billion years ago, such expansion being the longstanding interpretation of the clearly-observed monotonically-increasing redshift of galaxies as a function of their distance. That premise was initiated with interpretation of the Einstein field equations (EFE) in the context of cosmology by [Friedman \(1922\)](#) and [Lemaître \(1927\)](#), which not only gave credence to the expanding universe model, but also precluded a ‘static’ universe model of fixed volume, currently understood to be a physical impossibility. When [Hubble \(1929\)](#) claimed

empirical discovery of a linear galaxy redshift-distance relationship consistent with such expansion, this met the existing expectations of the budding theoretical cosmology community. Thus, the paradigm of an expanding universe was born from the apparent confluence of theory and empirical evidence.

Hubble’s 1929 galaxy redshift-distance graph claimed evidence for a constant expansion rate of $H_0 \approx 500 \text{ km s}^{-1} \text{ Mpc}^{-1}$. Actually, there was no real “discovery”; Hubble effectively drew a random straight line through sparse and inaccurate redshift-distance data that supported an existing theoretical proposal of such relationship, of which he then and thereafter professed to have no prior knowledge. That deception, which was a **typical idiosyncratic behavior pattern** as revealed in various biographies, gave the illusion of unbiased interpretation of objective data constituting a major empirical discovery. Hubble did not cite [Lemaître \(1927\)](#), which proposed cosmic expansion with $H_0 \approx 625$, yet there is compelling evidence that Hubble’s claimed independent discovery was motivated

by familiarity with Georges Lemaître’s theory of a linear galaxy redshift-distance relationship and its implications for a “moment of creation,” giving scientific credence to Lemaître’s personal interpretation of biblical *Genesis* 1:1 [Kragh \(2004\)](#); Georges Lemaître first visited Edwin Hubble at Mt. Wilson in June 1925 [Farrell \(2005\)](#); a second meeting occurred at the 1928 IAU conference in Holland [van den Bergh \(2011\)](#). It shall be made self-evident that similar fabrication of evidence supporting prevailing theory has persisted to date; the conventional trust the scientific community puts on the reliability of claimed ‘empirical data’ to guide objective scientific judgement is not justified in the case of the historical development of present-day (c. 2019) canonical cosmology.

This paper presents compelling new theory and reliable, corroborating empirical evidence overthrowing the current paradigm in cosmology, and it reveals parallels between the ill-founded solar system model of antiquity and that current standard model. Herein we correct a succession of scientific errors associated with [confirmation bias](#); it is established beyond doubt that galaxy redshifts are presently misinterpreted.

2 | A SIMPLE COSMOLOGICAL MODEL

In order for a physical model to provide a correct representation of empirical reality, it must be based on the fundamental underlying physical principle (e.g., a heliocentric solar system model, versus the absurd Geocentric model of antiquity that was based on the illusion of a stationary Earth orbited by the Sun, planets, and stars). Similarly, Sean Carroll’s apt URL, [preposterousuniverse.com](#), is motivated by the absurd recent notion that ~95% of the universe is ‘dark’ [energy and matter](#), associated with the prevailing interpretation of galaxy redshifts as *accelerating* cosmic expansion. Evinced by the long history of Geocentrism, no amount of time or effort expended on a physical model with a fallacious underlying assumption will result in sound scientific understanding of phenomena.

2.1 | A rational foundation

A sound cosmological model is based on the singular rational foundation of a finite, boundaryless, symmetric cosmic volume incorporating a universally-conserved amount of mass-energy; no other approach can be fruitful. Translated into the language of pure mathematics (i.e., *geometry*) such a volume constitutes a Riemannian topological *3-sphere*, having a total volumetric bounding area of $2\pi^2 R^3$ and a closed spatial geodesic, which is the circle C of circumference $2\pi R$. The indirectly-measurable Cosmic radius R may be conveniently normalized.

2.2 | The geometry of time

Although special relativity (SR) incorporates the idealized conception of ‘flat’ spacetime, that idealization holds to high accuracy for an arbitrarily-small volume of space in free fall. In accord with the [Minkowski \(1909\)](#) metric, we model such a differential volume with four basis vectors, one of which represents the *local* proper time coordinate (i.e., representing a valid physical measurement exclusively within the volume of space bounded by the other three basis vectors.) As such, the local proper time coordinate is clearly a *geometric object*, being the local normal in R^4 to measurable 3-space in free fall.

2.3 | Synthesis

Combining the two fundamental ideas from [2.1](#) and [2.2](#), yields a parsimonious geometric model of the Cosmos. Two of the three spatial dimensions being suppressed, it incorporates a single dimension of *local* space that is given maximum cosmological extension (i.e., the circle C) and also a strictly-local relativistic time coordinate: At each unique point on C , the local radial (i.e., the local normal to space) represents the local proper time coordinate there. The inherent non-parallelism between any two such local-time-coordinate vectors reflects a symmetric relativistic time dilation between their respective locations that is quantified by the inverse dot product

$$\frac{dt}{d\tau} = \frac{1}{\cos \chi} = \sec \chi \quad \left(\angle \chi = \frac{r}{R} \right), \quad (1)$$

where r is the distance between a reference observer on C with local proper time coordinate dt and a remote location with distinct local proper time coordinate $d\tau$. As in SR, the relationship is symmetric; there are no preferred locations on C .

Given the definition of redshift induced by time dilation

$$z = \frac{dt}{d\tau} - 1, \quad (2)$$

then combining Eqs. (1) and (2) yields a distinctly non-linear redshift-distance relationship:

$$r(z) = R \cos^{-1} \left(\frac{1}{z+1} \right) \quad (3)$$

A likely initial subjective ‘problem’ with this predictive formula is the obvious conflict with decades of published data, having small error bars and claiming to confirm a linear redshift-distance relationship in support of the ‘Hubble law.’ According to all of that prior literature, Eq. (3) is patently incorrect, yet at one time a similar majority opinion, supported by centuries of academic literature, held for heliocentric orbits. It shall be determined from modern, objective, statistically-significant astrophysical data that Eq. (3) and correlated predictive formulas provide an essentially perfect fit to that data. Contrariwise, the prior literature is shown to reflect confirmation bias, and the ‘Hubble law’ is definitively falsified.

2.4 | The de Sitter metric

In rebuttal to (Einstein, 1917), de Sitter (1917a) made an insightful criticism:

We thus find that in [Einstein's metric] the time has a separate position. That this must be so, is evident a priori. . . . Such a fundamental difference between the time and the space-coordinates seems to be somewhat contradictory to the complete symmetry of the field-equations . . .

The criticized precursor metric is identical to Eq. (4), with the exception of being absent the $\cos^2(r/R)$ term in the time component, these equations being found in this more intelligible form in (de Sitter, 1917b). That cosine term $f(r)$ correlates the measurement of time ($d\tau = ds/c$) by an ideal clock at a remote location to measurement of reference “coordinate time” (dt) by a similar local clock as a function of fixed radial distance r between the two clocks. Without that term, there is no such correlation, which results in a non-relativistic *universal time coordinate* (i.e., ‘Cosmic Time’ from initial singularity) shared by all observers within the total cosmological volume of space defined by the metric.

$$ds^2 = -dr^2 - R^2 \sin^2 \frac{r}{R} (d\psi^2 + \sin^2 \psi d\theta^2) + \cos^2 \frac{r}{R} c^2 dt^2 \quad (4)$$

For fixed distance r between observers ($dr = d\psi = d\theta = 0$),

$$ds^2 = \cos^2 \frac{r}{R} c^2 dt^2 \quad \rightarrow \quad d\tau = \cos \frac{r}{R} dt, \quad (5)$$

which is identical to Eq. (1), the former equation having been derived independently of the EFE from simple geometric considerations, which include the mathematical foundations of relativity (i.e., the Minkowski metric) and Riemann (1854).

Both (Einstein and de Sitter) solutions of the EFE involve a non-zero cosmological constant. A distinct peculiarity of the de Sitter metric is that it requires a *zero average* cosmic matter density ($\rho_0 = 0$), which was naïvely interpreted as indicative of an unphysical “empty universe”; thus it was historically abandoned as nothing more than a mathematical curiosity.

2.5 | Cosmological relativistic time reversal

Normalizing the Cosmic radius R , so that r is a radial distance measured in radians, Eq. (5) is more simply expressed as

$$\frac{dt}{d\tau} = \frac{1}{\cos r} = \sec r \quad [0 \leq r \leq \pi]. \quad (6)$$

At finite distance $r = \pi/2$ from an arbitrarily-located observer, the time dilation factor, comparing the rate of the observer's ideal reference clock to a similar remote clock, is indeterminate; at this distance the remote clock is effectively stopped relative to the observer's clock. That boundary represents that

observer's “cosmological redshift horizon”; no information about the other half of the Universe is available to the observer. Over the spatial interval $[\pi/2 \leq r \leq \pi]$ the time dilation factor is negative and -1 at the observer's cosmological antipode. This inherent time reversal between cosmological antipodes is a relativistic effect whereby the known laws of physics, such as the second law of thermodynamics, are the same everywhere. However, given the inherent symmetry of the phenomenon, there is an important systemic energy consequence:

The cosmological principle requires the mass-energy density of the Universe to be uniform on large distance scales; accordingly, any two halves of the Universe, with arbitrarily-chosen separation boundary, each have the same number of baryons, likely not more than $N \sim 10^{81}$. Also, in the context of relativistic physics, *time reversal yields negative energy*. From a synthesis of these two principles one may infer that, according to any observer, the *net* energy of the Universe is *zero* in the context of relativistic physics. Normalizing the arbitrary magnitude of the positive mass-energy content of the observer's visible half of the Universe, the trivial relativistic energy equation yielding this *zero* net cosmic energy is the sum $1 + (-1) = 0$. Certainly, this *zero* net energy value is consistent with a *zero average* cosmic matter density ($\rho_0 = 0$), but this does not entail that the Universe is devoid of matter, for the equation necessitates an equal positive value of N baryons ($\rho_1 = \rho_2 = \frac{N}{\pi^2 R^3}$) for each of the two summed components.

2.6 | Cosmological topology

Seeking a solution to the EFE yielding a cosmological metric in accord with “the complete symmetry of the field-equations,” de Sitter was on the right track and he clearly succeeded, yet nobody had an intuitive understanding of the physical interpretation of the mathematics. As related by Heisenberg, Einstein is quoted as saying in 1926, “Only the theory decides what one can observe” Holton (2000). Given the expanding-universe theory, which became increasingly favored over subsequent decades, almost everybody ‘observed’ what they already believed in—an expanding universe; what they did *not* observe was empirical reality. That is about to change. . .

In hindsight, a sure sign of the primitive nature of the present-day standard cosmological model is its simplistic assumption of a Euclidean space, whereby the volume of enclosed space increases with the square of the radial distance. This is akin to the irrational ‘flat Earth’ model, prevalent before the Common Era in Western culture. To make matters worse, we have a celebrated latter-day “Science Team” who boldly claim to have “nailed down the curvature of space to within 0.4% of “flat” Euclidean.” It is hard to argue with a group of experts (WMAP Science Team) claiming that level of certainty using a \$150M spacecraft; nevertheless, I beg to differ. . .

Where the point designated $\chi = 0$ represents the location of the Milky Way (i.e., an arbitrary cosmic point of reference), the S^2 hemisphere shown in Fig. 1 is a representation of an arbitrary 2-dimensional slice of the *observable* Universe, such as the extended plane of the Galaxy. The Cosmic radius is static ($\dot{R} = 0$). The unique local normal (i.e., radial vector) at every point on the surface represents the distinct local proper time at that point. Observation of a distant galaxy occurs over the measured distance r . As per Eqs. (1) and (2), the measured static-distance-induced redshift of the observed galaxy is

$$z = \sec \chi - 1. \quad (7)$$

Due to the curvature of space, the apparent angular size of the galaxy is inversely proportional to the radius ρ , where

$$\sin \chi = \rho/R. \quad (8)$$

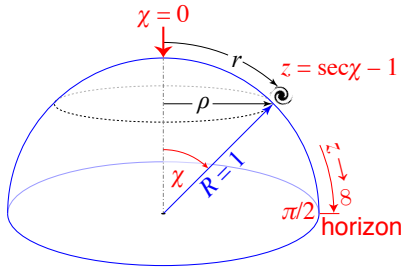


FIGURE 1 A 2D slice of the observable Universe, the other half (beyond the z -horizon) being inherently unobservable. This model's elegant simplicity heralds its predictive power.

2.7 | New predictive equations

The set of interdependent predictive equations for standard astrophysical observables complementing Eq. (3) follow immediately from the geometry of the Riemannian 3-sphere. All are similarly-elegant analytic functions exclusively of measured redshift (z). For absolute measurements, the single free parameter employed by the new Riemannian-cosmic-geometry predictive formulas is the cosmic radius R . The value of this parameter can be estimated to close approximation from the theta- z formula (11) in conjunction with empirical observation of galaxy nuclei, which prove to function as reliable cosmic standard rods. For relative measurements, those formulas have no free parameters; the distinct variable C_{\square} appearing in each formula is just an arbitrary data-dependent scaling constant, (e.g., for redshift-magnitude its value depends on the intrinsic brightness of the specific standard candle under consideration). Due to this paper's limited page space, the detailed derivation steps for each formula are presented [externally](#).

Formulas

redshift-volume (arbitrary units)

$$S^3(z) = \text{volumetric 'surface' of a 3-sphere} \quad (9)$$

$$C_V \cdot 2\pi \left[\cos^{-1} \left(\frac{1}{z+1} \right) - \left(\frac{1}{(z+1)^2} - \frac{1}{(z+1)^4} \right)^{\frac{1}{2}} \right]$$

volume element (arbitrary units)

$$\frac{dS^3}{dz} = \quad (10)$$

$$C_{dV} \cdot \frac{4\pi}{\sqrt{1-(z+1)^{-2}}} \left(\frac{1}{(z+1)^2} - \frac{1}{(z+1)^4} \right)$$

theta- z (radians)

$$\theta(z) = C_{\delta} \left(1 - \frac{1}{(z+1)^2} \right)^{-\frac{1}{2}} \quad (11)$$

redshift-magnitude (mags)

$$m(z) = C_M - 2.5 \cdot \log \left(\frac{1}{4\pi [(z+1)^4 - (z+1)^2]} \right) \quad (12)$$

3 | CONFRONTATION WITH SDSS DATA

The Sloan Digital Sky Survey is currently in its fourth phase of operation (SDSS-IV) [Blanton et al. \(2017\)](#), having made its 14th cumulative data release (DR-14) [Abolfathi et al. \(2018\)](#). The survey, which began operation in 1998, employs a unique 2.5-meter telescope [Gunn et al. \(2006\)](#) located at Apache Point, New Mexico. With DR-7 [Abazajian et al. \(2009\)](#) and the close of SDSS-II, the spectra of over 800k galaxies and 100k quasars had been measured. SDSS-III, which ran from 2008–2014 and culminated in DR-12 [Shadab et al. \(2015\)](#), included a new near-infrared high-resolution spectrograph and other upgrades. There are now over 2M galaxy spectra in the SDSS database. This paper's long-term research effort first made use of SDSS data in 2005 using DR-4 [Adelman-McCarthy et al. \(2006\)](#). All SDSS data presented in this paper is from the most current database release available in 2018 (DR-14), dated July 2017.

Complementing high-quality measurements for galaxy redshift, size, and magnitude, each of which includes an error estimate, a principal advantage of the SDSS survey is the large volume of data, which covers over 35% of the sky and extends to high redshift. Even after applying stringent quality standards by restricting measurement-errors to small values, the typical data pool is on the order of 1M galaxies. In addition, measurements are made through five different astronomical filters (u, g, r, i, z), so for each target galaxy within the database,

there are actually five distinct data points for each empirical value, such as various magnitudes and radius measurements. In 2013, Prof. Mike Blanton of NYU described the ongoing [SDSS research effort](#) as, “This is one of the biggest bounties in the history of science.” A second advantage of SDSS data is that it reflects the primary mission objective to measure the empirical properties of galaxies, and not to prove any preconceived physical theory. As concerns that raw data, this theory-free agenda avoided the common problem pointed out by Einstein, whereby strongly-held preconceived notions tend to severely limit our perception of empirical reality.

3.1 | Theta-z data

Averaging half-light radius measurements over three bandpass filters $\{g, r, i\}$ and ensuring that no individual radius measurement has greater than 20% error (1% for z) provides for the exceptionally high-quality Fig. 2 theta-z dataset. See the figure caption for details. The set of six z -bins represent $\sim 365k$ individual radius measurements for $\sim 122k$ galaxies.

Using the $z=0.08$ bin, Fig. 3 demonstrates an observation that is similar for all of the bins: galaxies exhibit a log-normal size distribution. Also, from both Fig. 2 and Fig. 3 one may infer a decadal range in typical galaxy size, excluding statistically-improbable outliers. Fig. 3 references Eq. (13).

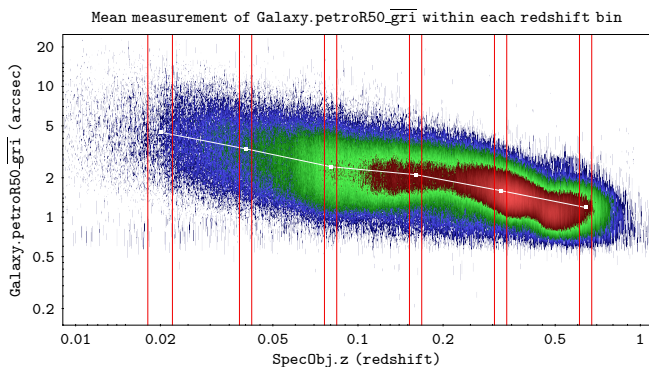


FIGURE 2 Half-light radius data averaged over $\{g, r, i\}$ for $\sim 755k$ galaxies ($\sim 2.3M$ data points). Individual measurement error limited to 20%. Dataset average measurement error 3.6%. Redshift-bin (0.02, 0.04, 0.08, 0.16, 0.32, 0.64) mean radius measurements shown as white squares. Red lines demarcate the six redshift-bins. The white line is intended as a visual aid. RGB color scheme denotes data density (high to low).

Probability Density Function (Fig. 3 gray curve):

$$f_x(\theta; \mu, \sigma) = \frac{1}{\theta\sigma\sqrt{2\pi}} e^u \quad \text{where} \quad u = -\frac{(\ln \theta - \mu)^2}{2\sigma^2} \quad (13)$$

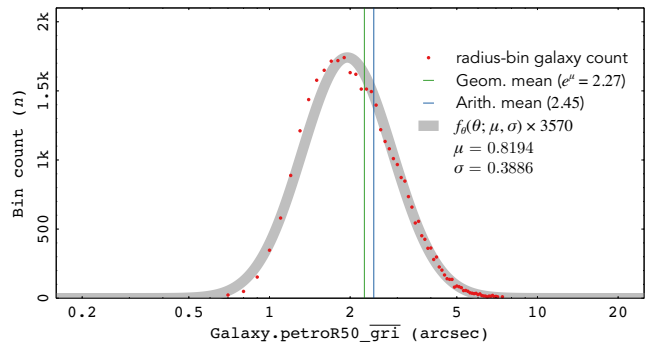


FIGURE 3 The data in red represents 35,985 galaxies with $\bar{z} = 0.080$ in bin ($0.076 \leq z \leq 0.84$), which clearly exhibit a near-perfect fit to the log-normal probability density function (gray curve) described by Eq. (13), parametrized by empirical dataset attributes (μ, σ) , where θ has values `petroR50_gri`.

The two parameters μ and σ are, respectively, the mean and standard deviation of the variable’s natural log (i.e., $\ln \theta$). Fig. 4 shows the unscaled (absent source data) PDF functions for all six bins, clearly demonstrating the effect of Malmquist bias on the measurement. With increasing redshift, smaller galaxies drop out of the sample. Also, the dim distal region of large galaxies is not seen with increasing redshift-bin distance, thus their radius measurement is less than for the same intrinsic size at lower redshift. Due to this ‘squeeze,’ the mean radius measurement is largely unbiased. Statistically, that mean measurement (Fig. 2) represents a “cosmic standard rod,” or a ubiquitous class of galaxy having the same intrinsic size.

The second column of the Fig. 4 legend indicates the bin galaxy count (N). The third column shows the arithmetic mean measurement ($\bar{\theta}$). For the three high-population bins, the fourth column shows the mean radius plus two standard deviations ($\bar{\theta} + 2\sigma$), which represents the class of unusually-large and easiest-to-measure galaxies in the bin.

According to the ‘Hubble law,’ at lower redshift, galaxies at $2z$ are twice the distance of those at z and the predicted observable is that they will be half the size. The statistical data in Fig. 4 is at odds with that prediction; it apparently falsifies that purported physical law.

Fig. 5 confronts the empirical SDSS theta-z data with both the Eq. (11) prediction and the Λ CDM model, using the current “consensus” values of that model’s primary free parameters. Also shown is a ‘Hubble law’ relationship (dashed curve), predicting exactly half the apparent size at double the redshift. With any modification of the standard model’s free parameters, the predictive curve must remain very nearly aligned to the dashed curve as seen here; this confrontation indicates a failure of the standard-model prediction. Contrariwise, the Eq. (11) curve in red provides a nearly perfect fit to the data and there

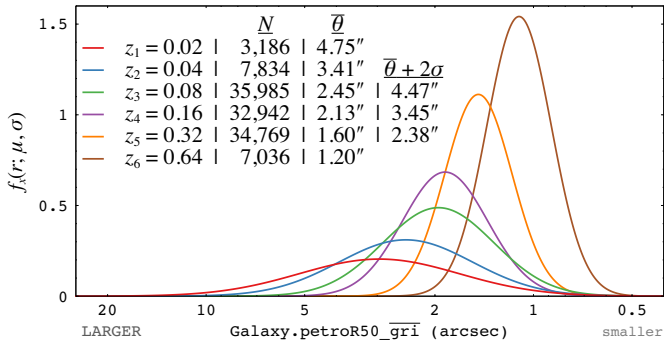


FIGURE 4 PDF functions for the six redshift bins based on determination of μ and σ for each bin using a database query.

are no free parameters to subjectively manipulate such a fit; objectively, the new a priori model is empirically accurate.

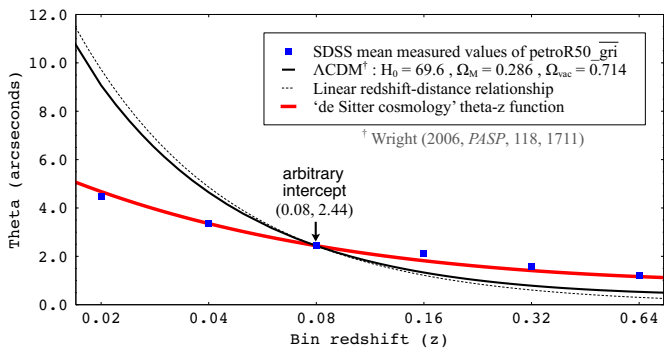


FIGURE 5 The red curve plots Eq. (11) with $C_\delta = 0.9216$ to set the intercept. The solid black curve is a plot of $763/D_A(z)$, where *Ned Wright's Javascript Cosmology Calculator* was employed to generate a set of ordered pairs (z, D_A) in accord with the Λ CDM consensus cosmological model. The constant 763 sets the intercept. There is no analytic function for the angular size distance, where the predicted apparent size of a standard rod of intrinsic size δ is defined: $\theta(z) = \delta/D_A(z)$.

3.2 | Redshift-magnitude data

Fig. 6 confronts the empirical SDSS redshift-magnitude data (z -band Petrosian magnitudes) with both the Eq. (12) prediction and the Λ CDM model using the ‘‘consensus’’ parameters. That model prescribes that $z = 0.03$ is 400M yrs ago and $z = 0.5$ is 5.1G yrs ago. Interpreting the Λ CDM standard-candle curve, five billion years ago, the brightest galaxies were more than ten times ($10\times$) brighter than in the current epoch due to an implausible accelerating dimming process that has

extinguished 90% of the stars. On the other hand, one can infer from the ‘de Sitter’ curve that the brightest galaxies in the Universe constitute a ubiquitous class of luminous object having a variation in intrinsic brightness of about ± 0.2 mag ($\pm 20\%$). It is obvious which curve represents a tenable physical model.

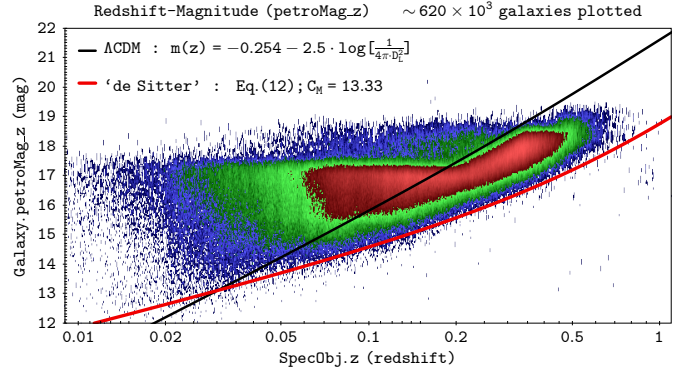


FIGURE 6 The red curve plots Eq. (12) with $C_M = 13.33$ to set the intercept. The solid black curve is a plot of $f(D_L)$ as per *CosmoCalc*-generated ordered pairs (z, D_L) . The constant -0.254 sets the intercept at $(0.03, 13.1)$. There is no analytic function for the luminosity distance. At $z=0.5$, the difference between the two curves is 2.57 mag (a factor of 10.7).

SDSS fiber magnitude data from the spectroscopic pipeline, which serendipitously measures the apparent brightness of galaxy nuclei, provides independent corroborating evidence. That data is presented externally so as to adhere to the page-length limitations imposed on this *IWARA Proceedings* paper.

3.3 | Galaxy space density

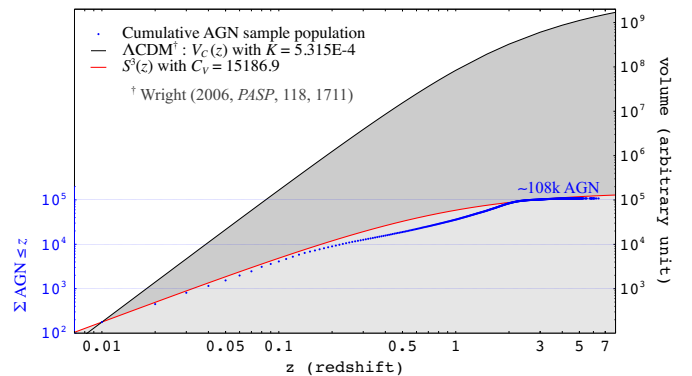


FIGURE 7 The data in blue, sourced from *NED* (73% SDSS), represents the cumulative AGN population in redshift space. The red curve plots Eq. (9); the black curve plots $K \frac{4\pi}{3} D_C^3$.

In Fig. 7, the arbitrary intercept for the two predictive curves is the first data point at $z = 0.01$. As per the caption, the Λ CDM comoving-volume curve is proportional to the cube of the comoving radial distance (D_C^3). A small percentage of galaxies host an active galactic nucleus (AGN), which has a much higher luminosity than normal; the brightest AGN are observed at very high redshift ($z > 6$), so these galaxies are an ideal observable with which to confront theoretical predictions of galaxy space density, including testable assumptions concerning galaxy evolution over lookback time. The correlation of the data to the red a priori ‘de Sitter’ curve is remarkable.

To reiterate, Eq. (9) has no free parameters that might be employed to fit the curve to any particular data set; it is exclusively a function of z . Confronting that curve with the data, the interpretation is clear: AGN are a ubiquitous, uniformly-distributed subset of the general galaxy population. One may also infer that there is no evolutionary process for AGN over lookback time, which is a strictly-local timescale.

The Λ CDM curve is unphysical; according to this fallacious model, the space density of AGN has increased by a factor of 10^4 over the last 13 Gyr, despite a modeled 8-fold increase in the scale factor since $z = 7$. Alternatively, assuming an empirical uniform AGN space density, the SDSS and complementary surveys are counting only about 1 out of 35 super-bright AGN at redshift 0.1, 1 out of 450 at redshift 0.5, etc., which is not a reasonable possibility.

4 | CONCLUSIONS

The Big-Bang theory is fallacious and is now falsified according to the tenets of modern professional science; the Universe is not expanding. Accordingly, all arguments that presume an expanding universe (e.g., the canonical explanation of the cosmic microwave background) are invalid. The vital field of cosmology is effectively ‘rebooted’ and there are decades of work ahead requiring thousands of innovative PhD theses worldwide related to physics and astrophysics.

Love truth but pardon error. – Voltaire

SUPPORTING INFORMATION

This *IWARA2018 Proceedings* paper has an imposed length limitation and thus includes limited detail. A self-study slide deck is available with additional information on this topic:

sensibleuniverse.net/slides

The September 2020 slide deck reflects very minor edits to the 2018/19 version.

EXCLUSION FROM PROCEEDINGS

This and the following section are addenda (c. May 2019) to the foregoing invited submission to the conference proceedings. They are intended to inform the reader about “How Physics and Astronomy Get Done” López Corredoira et al. (2008), and why this paper does not appear in those proceedings.

According to the conference organizer, the editor responsible for the *IWARA2018 proceedings*, comprising 251 pages in the January–March 2019 issues of *Astronomische Nachrichten*, was Prof. Thomas Boller. That publication included forty-nine articles by other conference presenters, with this paper having been excluded. The author was never contacted by the Proceedings editorial team, and there was no criticism or the opportunity to respond to such criticism. Expressing sorrow and encouragement, the conference organizer reported the editorial team’s following rationale: this paper “not included in the list of priorities that would allow its inclusion in the volume of the proceedings of the iwara2018 event.” (quote verbatim)

¶2 of §1 was slightly edited for this Sept. 2020 version.

VIDEO OF THE ORAL PRESENTATION

Initiated some minutes after the start of the author’s oral presentation at the conference, a graduate student attending the conference recorded this video of that presentation:

http://bit.ly/AFMayer_IWARA2018

REFERENCES

- Abazajian, K. N., et al. 2009, *ApJS*, 182(2), 543.
- Abolfathi, B., et al. 2018, *ApJS*, 235(2), 42.
- Adelman-McCarthy, J. K., et al. 2006, *ApJS*, 162(1), 38.
- Blanton, M. R., et al. 2017, *AJ*, 154(1), 28.
- de Sitter, W. 1917a, *KNAW Proc.*, 19(2), 1217.
- de Sitter, W. 1917b, *MNRAS*, 78, 3.
- Einstein, A. 1917, *SPAW*, 142.
- Farrell, J. 2005, New York: Thunder’s Mouth Press.
- Friedman, A. 1922, *Z. Phys.*, 10(1), 377.
- Gunn, J. E., et al. 2006, *AJ*, 131(4), 2332.
- Holton, G. 2000, *Phys. Today*, 53(7), 38.
- Hubble, E. 1929, *PNAS*, 15, 168.
- Kragh, H. 2004, London: Imperial College Press.
- Lemaître, G. 1927, *Ann. Soc. Scien. Bruxelles*, A47, 49.
- López Corredoira, M., et al. 2008, Boca Raton: Universal Publishers.
- Minkowski, H. 1909, *Jahresber. DMV*, 75.
- Riemann, G. F. B. 1854, *Nature*, 8(183, 184), 14, 36.
- Scott, D. 2018, *arXiv:1804.01318 [astro-ph.CO]*.
- Shadab, A., et al. 2015, *ApJS*, 219(1), 12.
- van den Bergh, S. 2011, *arXiv:1108.0709v2 [physics.hist-ph]*.
- Wright, E. L. 2006, *PASP*, 118, 1711.